The Innate Reactivity of a Membrane Associated Peptide Towards Lipids: Acyl Transfer to Melittin Without Enzyme Catalysis: Supporting Information

Robert H Dods,[‡a] Jackie A Mosely*[a] and John M Sanderson*[a]

Experimental Methods

Materials and sample preparation

Synthetic melittin (99.2% by HPLC, Batch No. L15686/b, Alexis brand) was obtained from from Enzo Life Sciences (Exeter, UK). Lipids were obtained as dry powders from Avanti Polar Lipids *via* Instruchemie B.V., The Netherlands.

The concentration of melittin in stock solutions was determined by absorbtion measurements at 280 nm, with the extinction coefficient calculated as 5570 M^{-1} cm^{-1}.[1]

All experiments were conducted in aqueous buffers at pH 7.4 containing sodium bicarbonate (10 mM) and sodium chloride (90 mM).

Liposomes were prepared by drying a solution of the lipid (typically 165 µl of a 2 mg/ml solution in $CHCl_3$) *in vacuo* to form a thin film around the side of a round bottomed flask. This film was then hydrated with 1 ml of buffer and after thorough mixing was subjected to five freeze thaw cycles. The vesicles were then extruded 10 times through laser-etched polycarbonate membranes (Whatman, 100 nm pore size) at 60 °C using a thermobarrel extruder (Northern Lipids, Burnaby, Canada) under a positive N_2 pressure.

Melittin acylation

Mixtures (52 µl) of melittin (46 µM) and liposomes (0.23 mM) were prepared by adding a solution of the peptide to each liposome dispersion in buffer. Following mixing, mixtures were incubated at 37 °C throughout each experiment. The pH values of the solutions (pH 7.4) were unchanged after mixing the peptide and liposomes. Control experiments were conducted using melittin without liposomes, and liposomes without melittin. For analysis by LC-MS, 5 µL of the reaction mixture was removed and diluted into 45 µL aqueous medium (20 mM ammonium bicarbonate at pH 7.4).

Tryptic digests

Calcium chloride (*aq*., 100 mM, 2.2 µl) was added to the melittin/liposome mixtures (20 µl). Trypsin solution (250 ng/µl, 0.025% acetic acid/50 mM Tris; 1 µl) was added. The mixture was agitated at 37 °C. After 18 h, samples were analysed by LC-MS.

LC-MS

LC MS was performed with a Surveyor HPLC coupled to an LTQFT MS (ThermoFinnigan Corp, Bremen, Germany). Chromatographic separation was achieved from 5 µL sample solution aliquots injected onto an Xbridge 3.5 µm C18, 100 x 2.1 mm column (Waters, Manchester, UK). The 12 minute reverse phase gradient conditions started at 95% (H_2O + 0.1 % formic acid) / 5 % (CH_3CN + 0.1 % formic acid) and finished at 5 % (H_2O + 0.1 % formic acid) / 95 % (CH_3CN + 0.1 % formic acid) with a mobile phase flow rate of 200 µL min^{-1}. Retention times were reproducible to within ±0.1 min. Photodiode array data were recorded over the wavelength range 200–600 nm. The positive ion electrospray signal was optimized: the nitrogen sheath gas was kept between 8–10 arbitrary units, the auxiliary gas and sweep gas were set between 2–4 arbitrary units, as per the manufacturer's software, the capillary was heated to 250 ºC and the spray voltage was held at 4.0 kV. The tube lens voltage was varied to deliver the optimal ion intensity. All full scan MS data were measured in the Fourier-transform ion cyclotron resonance mass analyser surrounded by a 7 Tesla superconducting magnet. All MS/MS experiments were performed by alternating between MS and MS/MS scans throughout the chromatographic run.

Isolation of the precursor ions for MS/MS was carried out in the linear ion trap with a fixed isolation window of 4 *m/z*. Collision-induced dissociation (CID) experiments were performed entirely within the linear ion trap using helium as a collision gas and an optimised normalised collision energy level of 25%. MS Data were recorded using the acquisition software Xcalibur version 2.0.7 (ThermoFisher Corp, Bremen, Germany) and processed using the embedded program Qual Browser. Further processing and preparation of figures was done using the XCMS package[2] in the the R Statistical Programming Environment (version 2.13.2).[3]

Blank Runs

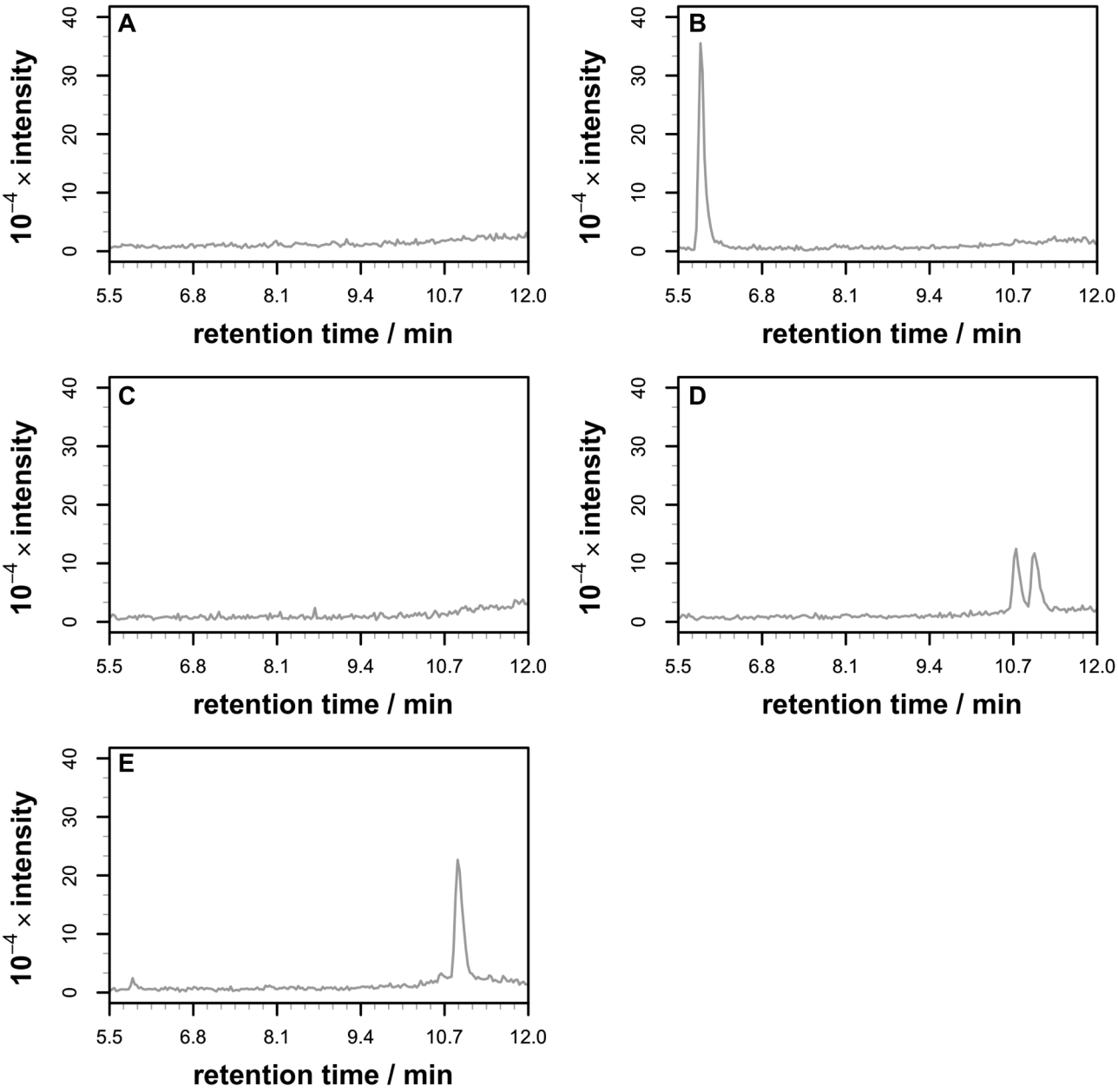

Fig. S1 LC chromatograms from blank runs, plotted as absolute intensity. (A) buffer only; (B) melittin only (no liposomes); (C) DOPC/DMPG liposomes in buffer after 4 h; (D) POPC liposomes, after 52 h; (E) DOPC/DMPG liposomes, after 52 h.

The only notable feature is the appearance of *lyso*-PCs in all samples after 2-3 days. Note that the ion currents for the *lyso*-PCs in the absence of melittin (Fig. S1D, Fig. S1E) are two orders of magnitude lower than those found in the presence of melittin (Fig. 1, main paper). Intensities for *lyso*-PCs were not used for quantification of the extent of reaction.

Data Filtering

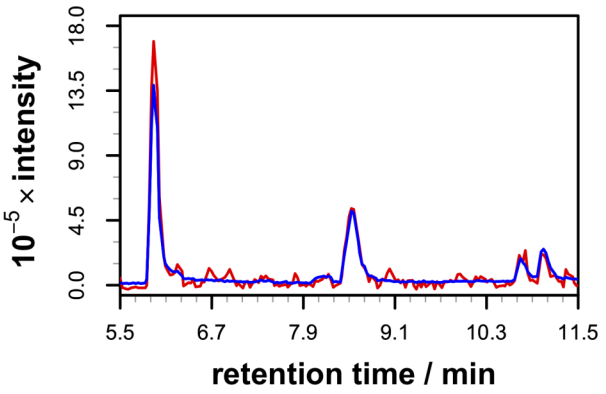

Fig. S2 Total ion current (red) and filtered ion current (blue) for POPC/melittin after 52 h, plotted as absolute intensity.

For the figures in the main paper, ion current data were filtered by combining the extracted ion currents (EICs) for all of the charge states of melittin, acylated melittin and *lyso*-PCs. This gave improvements in signal-to-noise ratio. Fig. S2 demonstrates that the combined EICs recapture the total ion current (TIC) for the peaks in the chromatogram (*i.e.* data are not being lost during filtering).

Double Peaks for *lyso*-PCs

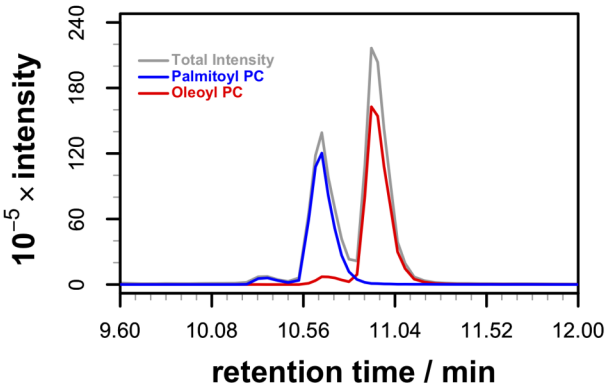

Fig. S3 *lyso*-PC section of the LC chromatogram from POPC/melittin after 52 h showing the TIC in this region and the EICs for both *lyso*-PCs, plotted as absolute intensities.

Each *lyso*-PC gave rise to two peaks in the chromatogram, one for the 1-acyl, and one for the 2-acyl. The intensity difference between the *lyso*-PC peak and the total intensity is due to doubly acylated melittin.

Peak Areas: Ion Current *vs* PDA

Table S1 Peak areas from the photodiode array detector and TIC chromatograms (see Fig. 1, main text).

	Peak Area (% of Total)[a]		Peak Area (% of Acyl Melittin)[a]	
	PDA	Ion Current	PDA	Ion Current
Melittin (peak i)	81	67	-	-
N-acyl (peak vi)	9	23	47	69
K23-acyl (peak v)	5	6	24	18
K7-acyl (peak iv)	1	1	3	5
K21-acyl (peak iii)	3	2	20	5
S18-acyl (peak ii)	1	1	6	4

[a] Peak areas were determined by fitting of an exponentially modified Gaussian function to the data.

Additional MS Data (Melittin + POPC)

Full spectra for main peaks

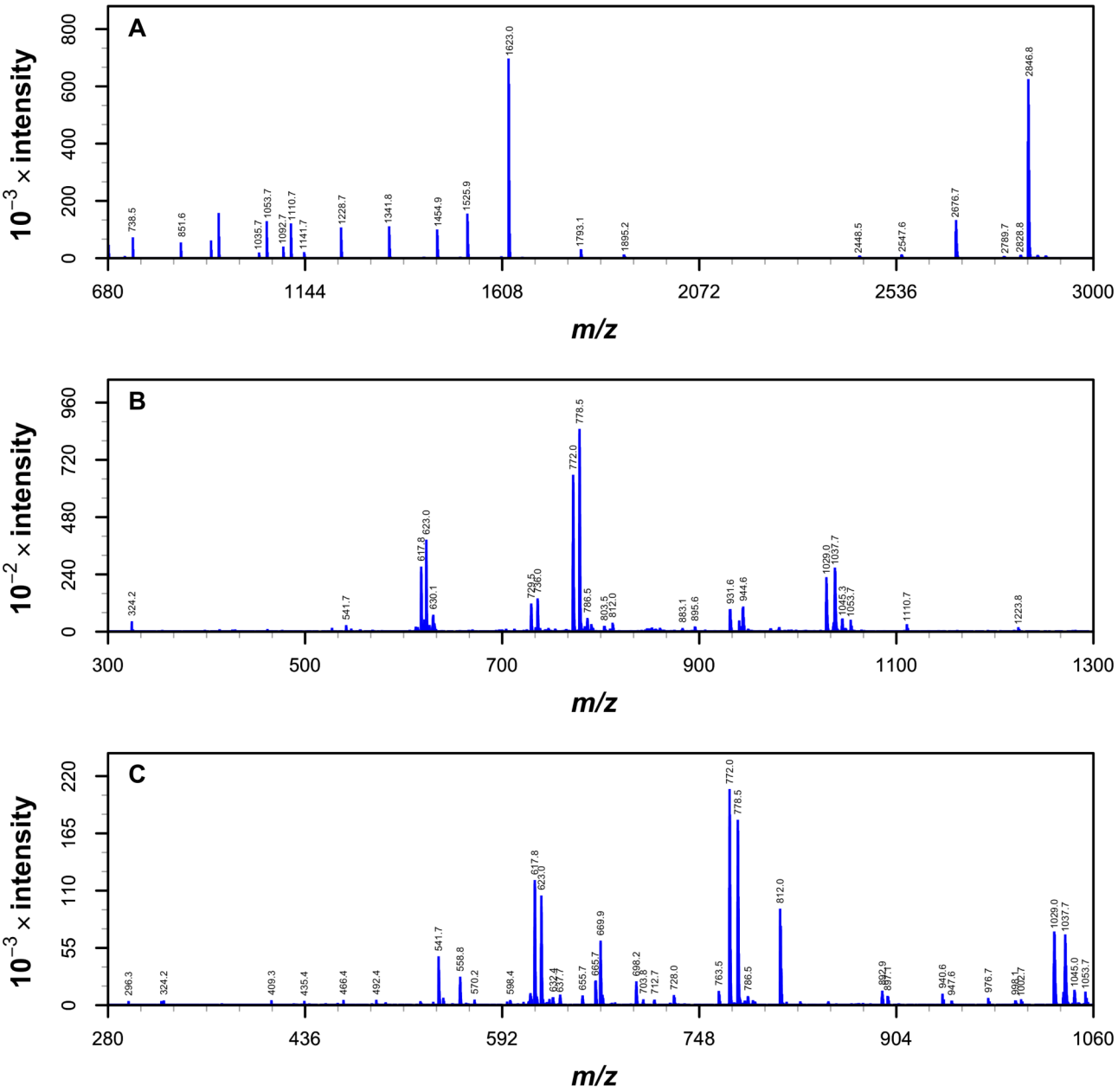

Fig. S4 Full MS spectra. MS spectra (absolute intensities) summed over peak i (A), peak v (B) and peak vi (C) of the LC trace in Fig. 1 (main paper). {(B) and (C) are full-scan versions of Fig. 2(A) and Fig. 2(B) of the main paper; (A) is deconvoluted to $[M + H]^+$}. Peak assignments are presented below in Tables S2-S4.

Table S2 Assignments for ions in the MS spectrum of peak i from the LC-MS trace of POPC/melittin (Fig. 1, main paper). These are the assignments for Fig. S4(A) and correspond to melittin.

ion[a]	Obs. *m/z*	*z*	sequence
$[Mel + H]^+$	2845.8	1	
b_{26} or $[Mel - H_2O]^+$	2827.8	1	
y_{25}	2788.7	1	IGAVLKVLTTGLPALISWIKRKRQQ-NH_2
y_{24}	2675.7	1	GAVLKVLTTGLPALISWIKRKRQQ-NH_2
y_{23}	2547.6	1	AVLKVLTTGLPALISWIKRKRQQ-NH_2
y_{22}	2448.5	1	VLKVLTTGLPALISWIKRKRQQ-NH_2
y_{16}	1894.2	1	TGLPALISWIKRKRQQ-NH_2
y_{15}	1793.1	1	GLPALISWIKRKRQQ-NH_2
y_{13}	1623.0	1	PALISWIKRKRQQ-NH_2
y_{12}	1525.9	1	ALISWIKRKRQQ-NH_2
y_{11}	1454.9	1	LISWIKRKRQQ-NH_2
y_{10}	1341.8	1	ISWIKRKRQQ-NH_2
y_9	1228.7	1	SWIKRKRQQ-NH_2
y_8	1141.7	1	WIKRKRQQ-NH_2
b_{12}	1110.7	1	GIGAVLKVLTTG
b_{12}-H_2O	1092.7	1	GIGAVLKVLTTG
b_{11}	1053.7	1	GIGAVLKVLTT
b_{11}-H_2O	1035.7	1	GIGAVLKVLTT
b_9	851.6	1	GIGAVLKVL
b_8	738.5	1	GIGAVLKV

[a] Key: Mel, melittin

Table S3 Assignments for ions in the MS spectrum of peak v from the LC-MS trace of POPC/melittin (Fig. 1, main paper). These are the assignments for Fig. S4(B) and correspond to K23-acylated melittin.

ion[a]	Obs. *m/z*	Calc. *m/z*	*z*	sequence[a]
b_{13}	1223.77	1223.77	1	GIGAVLKVLTTGL
b_{12}	1110.69	1110.69	1	GIGAVLKVLTTG
$[(Mel + Ol –H) + 3H]^{3+}$	1037.34	1037.34	3	
$[(Mel + Pal – H) + 3H]^{3+}$	1028.67	1028.67	3	
b_{11}	1053.67	1053.67	1	GIGAVLKVLTT
y_{13}	944.13	944.12	2	PALISWIKRKRQQ-NH_2 [1×Ol]
y_{13}	931.12	931.11	2	PALISWIKRKRQQ-NH_2 [1×Pal]
y_{12}	895.60	895.60	2	ALISWIKRKRQQ-NH_2 [1×Ol]
y_{12}	882.59	882.59	2	ALISWIKRKRQQ-NH_2 [1×Pal]
y_{10}	803.54	803.54	2	ISWIKRKRQQ-NH_2 [1×Ol]
$[(Mel + Ol – H) + 4H]^{4+}$	778.26	778.26	4	
$[(Mel + Pal – H) + 4H]^{4+}$	771.75	771.75	4	
y_{24}	735.73	735.73	4	GAVLKVLTTGLPALISWIKRKRQQ-NH_2 [1×Ol]
y_{24}	729.23	729.23	4	GAVLKVLTTGLPALISWIKRKRQQ-NH_2 [1×Pal]
y_{13}	629.75	629.75	3	PALISWIKRKRQQ-NH_2 [1×Ol]
$[(Mel + Ol – H) + 5H]^{5+}$	622.81	622.81	5	
$[(Mel + Pal – H) + 5H]^{5+}$	617.60	617.60	5	

[a] Key: Mel, melittin; Ol, oleoyl; Pal, palmitoyl

Table S4 Assignments for ions in the MS spectrum of peak vi from the LC-MS trace of POPC/melittin (Fig. 1, main paper). These are the assignments for Fig. S4(C) and correspond to N-acylated melittin.

ion[a]	Obs. *m/z*	Calc. *m/z*	*z*	sequence[a]
$[(Mel + Ol – H) + 2H]^{2+}$	1555.51	1555.51	2	
$[(Mel + Pal – H) + 2H]^{2+}$	1542.50	1542.50	2	
$[(Mel + Ol – H) + 2H + Na]^{3+}$	1044.67	1044.67	3	
$[(Mel + Ol – H) + 2H + Na]^{3+}$	1036.00	1036.00	3	
$[(Mel + Ol – H) + 3H]^{3+}$	1037.34	1037.34	3	
$[(Mel + Pal – H) + 3H]^{3+}$	1028.67	1028.67	3	
b_8	1002.73	1002.73	1	GIGAVLKV [1×Ol]
y_{17}	998.10	998.10	2	TTGLPALISWIKRKRQQ-NH_2
b_8	976.72	976.72	1	GIGAVLKV [1×Pal]
y_{16}	947.58	947.58	2	TGLPALISWIKRKRQQ-NH_2
y_{15}	897.06	897.06	2	GLPALISWIKRKRQQ-NH_2
$[(Mel + Ol – H) + 4H]^{4+}$	778.25	778.25	4	
$[(Mel + Pal – H) + 4H]^{4+}$	771.75	771.75	4	
y_{12}	763.48	763.48	2	ALISWIKRKRQQ-NH_2
y_{11}	727.96	727.96	2	LISWIKRKRQQ-NH_2
y_{18}	703.43	703.43	3	LTTGLPALISWIKRKRQQ-NH_2
y_{25}	697.94	697.94	4	IGAVLKVLTTGLPALISWIKRKRQQ-NH_2
y_{24}	669.65	669.65	4	GAVLKVLTTGLPALISWIKRKRQQ-NH_2
y_{17}	665.74	665.74	3	TTGLPALISWIKRKRQQ-NH_2
y_{23}	655.42	655.42	4	AVLKVLTTGLPALISWIKRKRQQ-NH_2
y_{22}	637.66	637.66	4	VLKVLTTGLPALISWIKRKRQQ-NH_2
y_{16}	632.06	632.06	3	TGLPALISWIKRKRQQ-NH_2
$[(Mel + Ol – H) + 5H]^{5+}$	622.81	622.81	5	
$[(Mel + Pal – H) + 5H]^{5+}$	617.60	617.60	5	
y_{15}	598.37	598.37	3	GLPALISWIKRKRQQ-NH_2
y_{25}	558.55	558.55	5	IGAVLKVLTTGLPALISWIKRKRQQ-NH_2
y_{13}	541.67	541.67	3	PALISWIKRKRQQ-NH_2
b_3	492.38	492.38	1	GIG [1×Ol]
b_3	466.36	466.36	1	GIG [1×Pal]
b_2	435.36	435.36	1	GI [1×Ol]
b_2	409.34	409.34	1	GI [1×Pal]
b_1	322.27	322.27	1	G [1×Ol]
b_1	296.26	296.26	1	G [1×Pal]

[a] Key: Ol, oleoyl; Pal, palmitoyl

N-oleoyl melittin

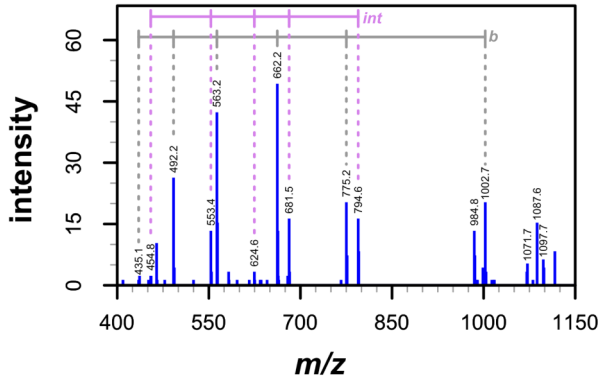

Fig. S5 MS^3 spectrum (absolute intensity) for N-oleoyl melittin in peak vi of the POPC chromatogram (Fig. 1 in the main paper). MS/MS precursor ion *m/z* 778; MS^3 precursor ion *m/z* 1115.5. This is the oleoyl equivalent of Fig. 3C in the main paper)

Table S5 Assignments for ions in the MS^3 spectrum of N-oleoyl melittin (Fig. S5)

ion	#	Obs. *m/z*	*z*	sequence[a]
b_8	8	1002.7	1	GIGAVLKV [1×Ol]
b_6	6	775.2	1	GIGAVL [1×Ol]
b_5	5	662.2	1	GIGAV [1×Ol]
b_4	4	563.3	1	GIGA [1×Ol]
b_3	3	492.2	1	GIG [1×Ol]
b_2	2	435.1	1	GI [1×Ol]
$b_8–H_2O$	8	984.8	1	GIGAVLKV [1×Ol]
$b_9–H_2O$	9	1097.7	1	GIGAVLKVL [1×Ol]
$b_9–CO$	9	1087.6	1	GIGAVLKVL [1×Ol]
$b_9–CO_2$	9	1071.7	1	GIGAVLKVL [1×Ol]
int	-	455.5	1	LKVL‡
int	-	553.4	1	VLKVL‡
int	-	624.6	1	AVLKVL‡
int	-	681.5	1	GAVLKVL‡
int	-	794.6	1	IGAVLKVL‡

[a] Key: M, melittin; Ol, Oleoyl; ‡ this is the closest match for this ion series, although the error between the observed and calculated *m/z* is 1 unit. This may be due to an uncharacterised rearrangement occurring due to the proximity of these residues to the oleoyl modification.

MS/MS data

Table S6 Assignments for ions in the MS/MS spectrum of peak vi (Fig. 1, main paper), precursor ion *m/z* 772.0 (assignments for Fig. 3(A) in the main paper).

ion	Obs. *m/z*	*z*	sequence[a]
y_{12}	763.2	2	ALISWIKRKRQQ-NH_2
y_{13}	812.8	2	PALISWIKRKRQQ-NH_2
y_{14}	868.8	2	LPALISWIKRKRQQ-NH_2
y_{15}	897.3	2	GLPALISWIKRKRQQ-NH_2
y_{16}	947.9	2	TGLPALISWIKRKRQQ-NH_2
y_{17}	998.5	2	TTGLPALISWIKRKRQQ-NH_2
y_{13}	542.1	3	PALISWIKRKRQQ-NH_2
y_{16}	632.4	3	TGLPALISWIKRKRQQ-NH_2
y_{17}	666.6	3	TTGLPALISWIKRKRQQ-NH_2
y_{21}	817.3	3	LKVLTTGLPALISWIKRKRQQ-NH_2
b_2	409.0	1	GI [1×Pal]
b_3	466.2	1	GIG [1×Pal]
b_4	537.2	1	GIGA [1×Pal]
b_5	636.3	1	GIGAV [1×Pal]
b_6	749.3	1	GIGAVL [1×Pal]
b_7	877.3	1	GIGAVLK [1×Pal]
b_8	976.6	1	GIGAVLKV [1×Pal]
b_9	1089.6	1	GIGAVLKVL [1×Pal]
b_{10}	1190.6	1	GIGAVLKVLT [1×Pal]
b_{12}	1348.7	1	GIGAVLKVLTTG [1×Pal]
b_{13}	1461.8	1	GIGAVLKVLTTGL [1×Pal]
b_7	439.4	2	GIGAVLK [1×Pal]
b_8	488.9	2	GIGAVLKV [1×Pal]
b_{10}	596.1	2	GIGAVLKVLT [1×Pal]
b_{13}	730.8	2	GIGAVLKVLTTGL [1×Pal]
b_{13}	488.9	3	GIGAVLKVLTTGL [1×Pal]
b_{18}	972.4	2	GIGAVLKVLTTGLPALIS [1×Pal]
b_{22}	844.6	3	GIGAVLKVLTTGLPALISWIKR [1×Pal]
b_{22}	632.4	4	GIGAVLKVLTTGLPALISWIKR [1×Pal]
b_{24}	703.7	4	GIGAVLKVLTTGLPALISWIKRKR [1×Pal]
b_{25}	980.7	3	GIGAVLKVLTTGLPALISWIKRKRQ [1×Pal]

[a] Key: Pal, palmitoyl

Table S7 Assignments for ions in the MS/MS spectrum of peak v, precursor ion *m/z* 778.5 (assignments for Fig. 3(B) in the main paper).

ion	Obs. *m/z*	*z*	sequence[a]
y_8	703.8	2	WIKRKRQQ-NH_2 [1×Ol]
y_9	747.2	2	SWIKRKRQQ-NH_2 [1×Ol]
y_{10}	803.8	2	ISWIKRKRQQ-NH_2 [1×Ol]
y_{11}	860.4	2	LISWIKRKRQQ-NH_2 [1×Ol]
y_{12}	895.9	2	ALISWIKRKRQQ-NH_2 [1×Ol]
y_{13}	944.4	2	PALISWIKRKRQQ-NH_2 [1×Ol]
y_{14}	1000.9	2	LPALISWIKRKRQQ-NH_2 [1×Ol]
y_{15}	1029.4	2	GLPALISWIKRKRQQ-NH_2 [1×Ol]
y_{16}	1080.0	2	TGLPALISWIKRKRQQ-NH_2 [1×Ol]
y_{17}	1130.5	2	TTGLPALISWIKRKRQQ-NH_2 [1×Ol]
y_{10}	538.0	3	l.ISWIKRKRQQ-NH_2 [1×Ol]
y_{13}	630.3	3	PALISWIKRKRQQ-NH_2 [1×Ol]
y_{14}	667.9	3	LPALISWIKRKRQQ-NH_2 [1×Ol]
y_{16}	720.4	3	TGLPALISWIKRKRQQ-NH_2 [1×Ol]
y_{17}	754.0	3	TTGLPALISWIKRKRQQ-NH_2 [1×Ol]
y_{20}	867.6	3	KVLTTGLPALISWIKRKRQQ-NH_2 [1×Ol]
y_{21}	905.3	3	LKVLTTGLPALISWIKRKRQQ-NH_2 [1×Ol]
y_{22}	938.4	3	VLKVLTTGLPALISWIKRKRQQ-NH_2 [1×Ol]
y_{23}	962.2	3	AVLKVLTTGLPALISWIKRKRQQ-NH_2 [1×Ol]
y_{24}	981.2	3	GAVLKVLTTGLPALISWIKRKRQQ-NH_2 [1×Ol]
y_{18}	594.6	4	LTTGLPALISWIKRKRQQ-NH_2 [1×Ol]
y_{24}	736.1	4	GAVLKVLTTGLPALISWIKRKRQQ-NH_2 [1×Ol]
b_6	511.2	1	GIGAVL
b_7	639.3	1	GIGAVLK
b_8	738.5	1	GIGAVLKV
b_9	851.6	1	GIGAVLKVL
b_{11}	1053.5	1	GIGAVLKVLTT
b_{12}	1110.6	1	GIGAVLKVLTTG
b_{13}	1223.6	1	GIGAVLKVLTTGL

[a] Key: Ol, oleoyl

Spectra for minor monoacylated products

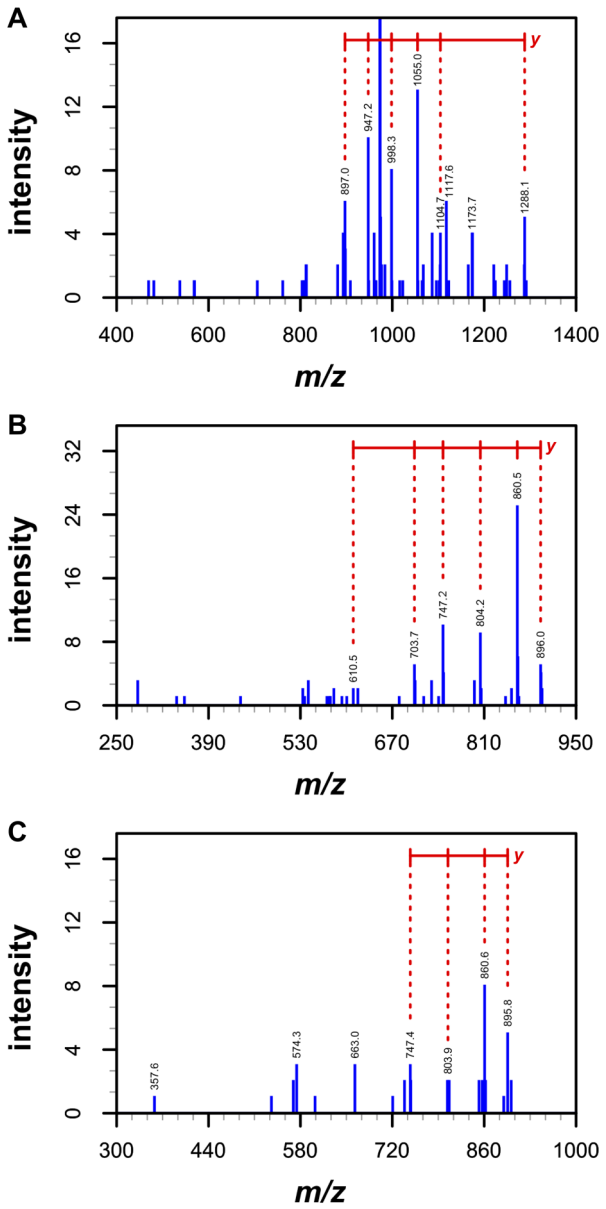

Fig. S6 MS spectra (MS^3) from the centre (maximum absolute intensity) of each of peaks ii, iii and iv (Fig. 1, main article). (A): peak iv, MS/MS precursor ion *m/z* 772, MS^3 precursor ion *m/z* 972; (B): peak iii, MS/MS precursor ion *m/z* 778, MS^3 precursor ion *m/z* 630.2; (C): peak ii, MS/MS precursor ion *m/z* 778, MS^3 precursor ion *m/z* 630.2.

Table S8 Identity of the MS^3 precursor ion with *m/z* 972 (Fig. 5(A), Fig. S6(A), Table S9).

ion[b]	Obs. *m/z*	Calc. *m/z*	*z*	sequence[a]
y	972.8	972.6	3	GAVLKVLTTGLPALISWIKRKRQQ–NH_2 [1×Pal]

[a] Key: Pal, palmitoyl; [b] this is the precursor ion for peaks ii–v in Fig 5(A) (main paper) and Table S9 (but ***not*** Tables S10 and S11)

Table S9 Assignments for ions in the MS^3 spectrum from the centre (maximum intensity) of peak iv (Fig. 1, main article). MS/MS precursor ion *m/z* 772, MS^3 precursor ion *m/z* 972; corresponds to Fig. S6(A).

ion[a]	Obs. *m/z*	*z*	sequence[a]
y_{20}	1288.1	2	KVLTTGLPALISWIKRKRQQ-NH_2 [1×Pal]
y_{19}	1104.7	2	VLTTGLPALISWIKRKRQQ-NH_2
y_{18}	1055.0	2	LTTGLPALISWIKRKRQQ-NH_2
y_{17}	998.3	2	TTGLPALISWIKRKRQQ-NH_2
y_{16}	947.2	2	TGLPALISWIKRKRQQ-NH_2
y_{15}	897.0	2	GLPALISWIKRKRQQ-NH_2

[a] Key: Pal, palmitoyl

Table S10 Assignments for ions in the MS^3 spectrum from the centre (maximum intensity) of peak iii (Fig. 1, main article). MS/MS precursor ion *m/z* 778, MS^3 precursor ion *m/z* 630.2; corresponds to Fig. S6(B).

ion[a]	Obs. *m/z*	*z*	sequence[a]
y_7	610.6	2	IKRKRQQ-NH_2 [1×Ol]
y_8	703.8	2	WIKRKRQQ-NH_2 [1×Ol]
y_9	747.2	2	SWIKRKRQQ-NH_2 [1×Ol]
y_{10}	803.8	2	ISWIKRKRQQ-NH_2 [1×Ol]
y_{11}	860.4	2	LISWIKRKRQQ-NH_2 [1×Ol]
y_{12}	895. 8	2	ALISWIKRKRQQ-NH_2 [1×Ol]
int	282.1	1	PAL

[a] Key: Ol, oleoyl; int, internal

Table S11 Assignments for ions in the MS^3 spectrum from the centre (maximum intensity) of peak ii (Fig. 1, main article). MS/MS precursor ion *m/z* 778, MS^3 precursor ion *m/z* 630.2; corresponds to Fig. S6(C).

ion[a]	Obs. *m/z*	*z*	sequence[a]
y_9	747.4	2	SWIKRKRQQ-NH_2 [1×Ol]
y_{10}	803.9	2	ISWIKRKRQQ-NH_2 [1×Ol]
y_{11}	860.6	2	LISWIKRKRQQ-NH_2 [1×Ol]
y_{12}	895.8	2	ALISWIKRKRQQ-NH_2 [1×Ol]
y_5	357.6	2	RKRQQ-NH_2

[a] Key: Ol, oleoyl

Doubly acylated melittin

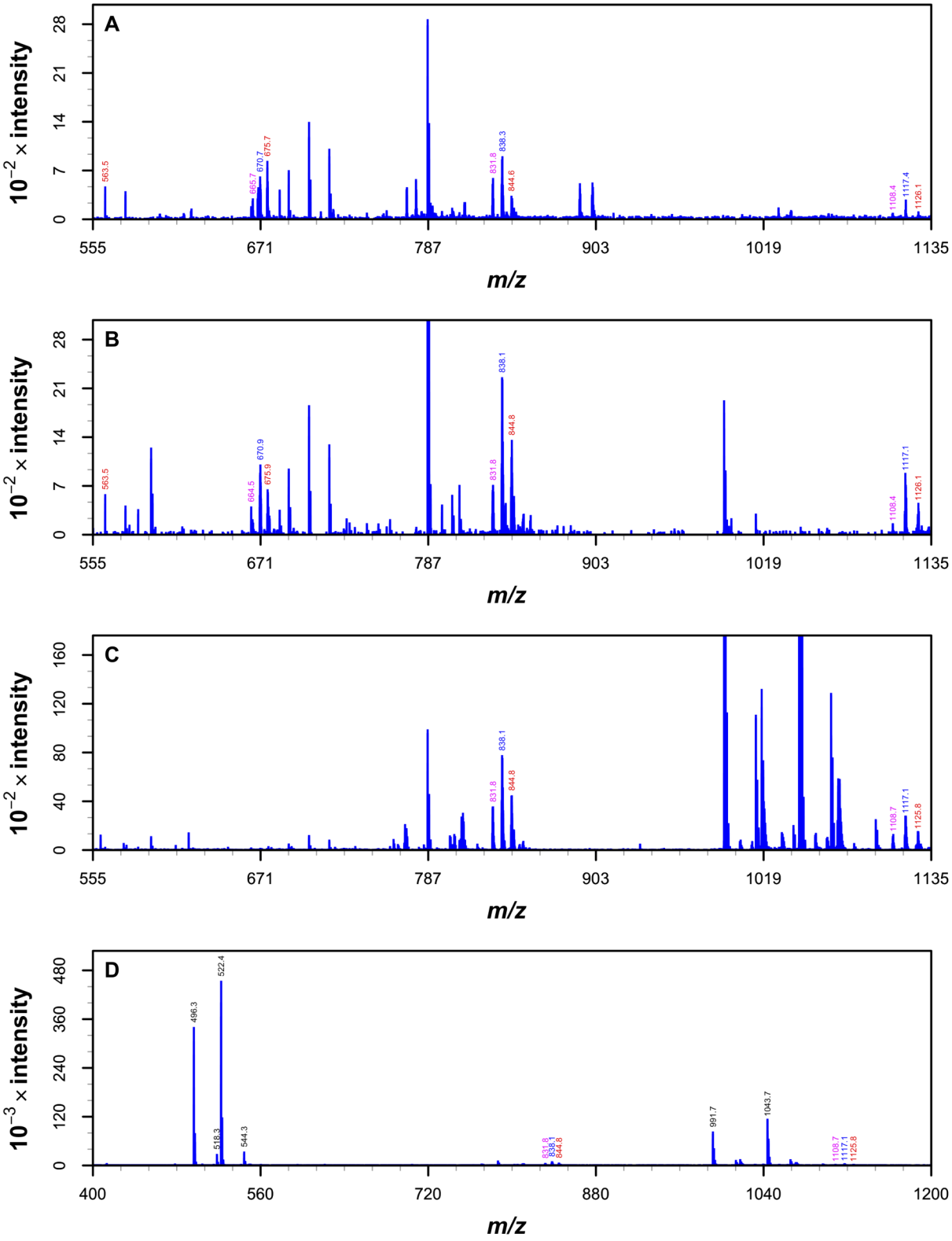

Fig. S7 MS spectra (absolute intensities) for doubly-acylated melittin. (A), RT range 9.3–9.7; (B), RT range 10.0–10.4; (C), RT range 10.4–11.4 (scaled to show doubly-acylated peaks); (D), RT range 10.4–11.4 (full y-range; main peaks are both *lyso*-PCs, plus their sodium adducts, and their proton dimers, see Table S12).

Table S12 Assignments for doubly acylated melittin (Fig. S7). Other data are given only for the main peaks in Fig. S7(A)–(D).

ion[a]	Obs. *m/z*	Calc. *m/z*	*z*
$[(Mel + 2Ol - 2H) + 3H]^{3+}$	1125.42275	1125.42221	3
$[(Mel + Ol + Pal - 2H) + 3H]^{3+}$	1115.75236	1116.75033	3
$[(Mel + 2Pal - 2H) + 3H]^{3+}$	1108.08106	1108.07844	3
$[(Mel + 2Ol - 2H) + 4H]^{4+}$	844.32010	844.31848	4
$[(Mel + Ol + Pal - 2H) + 4H]^{4+}$	837.81633	837.81457	4
$[(Mel + 2Pal - 2H) + 4H]^{4+}$	831.31244	831.31065	4
$[(Mel + 2Ol - 2H) + 5H]^{5+}$	675.65762	675.65624	5
$[(Mel + Ol + Pal - 2H) + 5H]^{5+}$	670.45455	670.45311	5
$[(Mel + 2Ol - 2H) + 5H]^{5+}$	665.24956	665.24998	5
$[(2 \times \text{mono-Oleoyl-PC}) + H]^{+}$	1043.70454	1043.70356	1
$[(2 \times \text{mono-Palmitoyl-PC}) + H]^{+}$	991.67352	991.67226	1
$[\text{mono-Oleoyl-PC} + Na]^{+}$	544.33856	544.33736	1
$[\text{mono-Oleoyl-PC} + H]^{+}$	522.35577	522.35542	1
$[\text{mono-Palmitoyl-PC} + Na]^{+}$	518.32273	518.32171	1
$[\text{mono-Palmitoyl-PC} + H]^{+}$	496.34007	496.33977	1

[a] Key: Mel, melittin; Ol, oleoyl; Pal, palmitoyl; PC, phosphocholine. All observed masses are accurate to within 3 ppm.

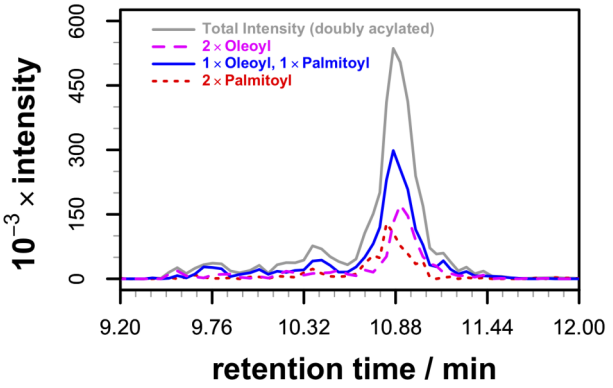

Fig. S8 Total and extracted ion intensities (absolute values) for doubly acylated melittin in the reaction with POPC after 52 h.

Tryptic digests of acylted melittin

Fig. S9(B) shows the mass spectrum of the most abundant lipidated peak in the digest profile, matching the sequence GIGAVLKVLTTGLPALISWIKR; *m/z* 849.2/1273.3 and 857.9/1286.3 correspond to $[M + 3H]^{3+}/[M + 2H]^{2+}$ for the palmitoylated and oleoylated peptides respectively. In addition, two ions are detectable with *m/z* 895.7 and 921.7 that correspond respectively to $[M + H]^{+}$ for the sequence GIGAVLK + palmitoyl and GIGAVLK + oleoyl. Fig. S9(C) shows the only other product detactable, GIGAVLKVLTTGLPALISWIK; *m/z* 797.2/1195.3 and 805.9/1208.3 correspond to $[M + 3H]^{3+}/[M + 2H]^{2+}$ for the palmitoylated and oleoylated peptides respectively.

These experiments were of necessity conducted with an excess of unreacted peptide present in the mixture, with the consequence that the detection of unmodified fragments could not be used to locate the positions of acylation. In addition, extensive digestion was not observed for the lipidated peptide, rendering the results from tryptic digests inconclusive. Nevertheless, the most abundant lipidated peptides (Fig S9(B) and (C)) are consistent with N-terminal acylation as a major product.

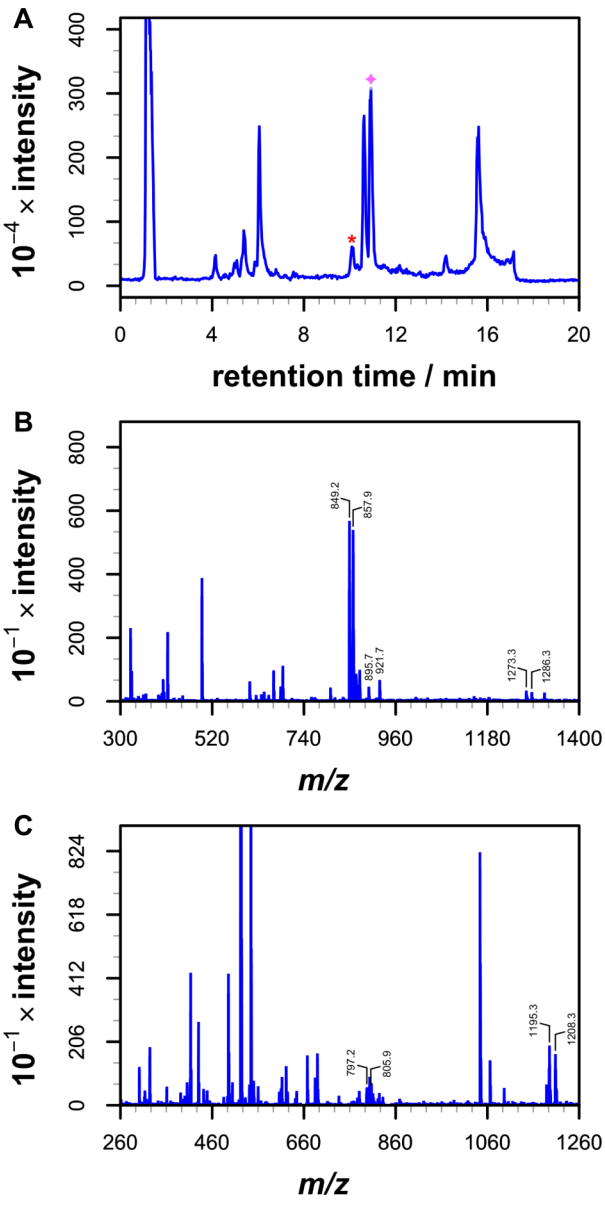

Fig. S9 (A) LC trace following trypsin digestion of a melittin/OPPC sample after 3 days incubation. The peaks indicated by an asterisk and a diamond contain acylated products (although the main component of the peak indicated with a diamond is 1-oleoyl-PC). (B) mass spectrum from the peak indicated by an asterisk; (C) mass spectrum of the peak indicated by a diamond. LC conditions as Fig. 1 (main article).

Reaction with DOPC/DPPS

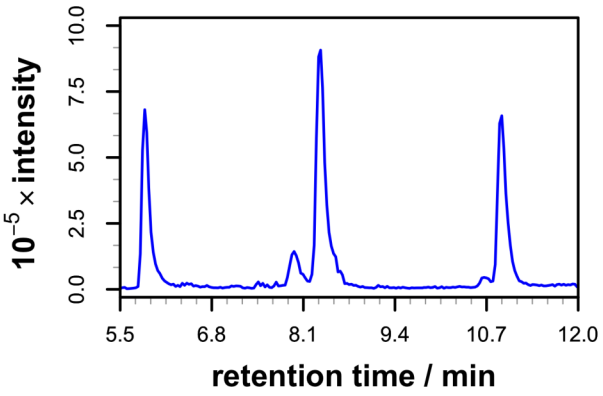

Fig. S10 TIC (absolute intensity) for the incubation of melittin (0.25 mM) with DOPC/DPPS(45 μM) at 37 °C in 10 mM $NaHCO_3$/90 mM NaCl, after 53 h. Separation was performed using an Xbridge C18, column (Waters, UK), with a linear gradient of 95% H_2O/5% MeCN to 5% H_2O/95% MeCN in 12 min.

Reaction with DOPC/DMPG

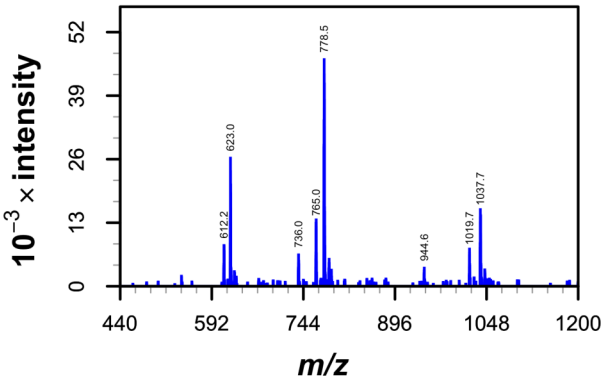

Fig. S11 Mass spectrum from peak iii of the melittin+DMPG/DOPC LC chromatogram (Fig. 9, main paper).

Table S13 Assignments for ions in the MS spectrum (Fig. S11, above) from peak iii of the DMPG/DOPC chromatogram (Fig. 9, main paper).

ion[a]	Obs. *m/z*	Calc. *m/z*	*z*	sequence[a]
$[(Mel + Myr - H) + 5H]^{5+}$	612.00	612.00	5	
$[(Mel + Ol - H) + 5H]^{5+}$	622.81	622.81	5	
y_{24}	735.73	735.73	4	GAVLKVLTTGLPALISWIKRKRQQ-NH_2 [1×Ol]
$[(Mel + Myr - H) + 4H]^{4+}$	764.75	764.75	4	
$[(Mel + Ol - H) + 4H]^{4+}$	778.26	778.26	4	
y_{13}	944.13	944.12	2	PALISWIKRKRQQ-NH_2 [1×Ol]
$[(Mel + Myr - H) + 3H]^{3+}$	1019.32	1019.32	3	
$[(Mel + Ol - H) + 3H]^{3+}$	1037.34	1037.34	3	

[a] Key: Mel, melittin; Myr, myristoyl; Ol, oleoyl

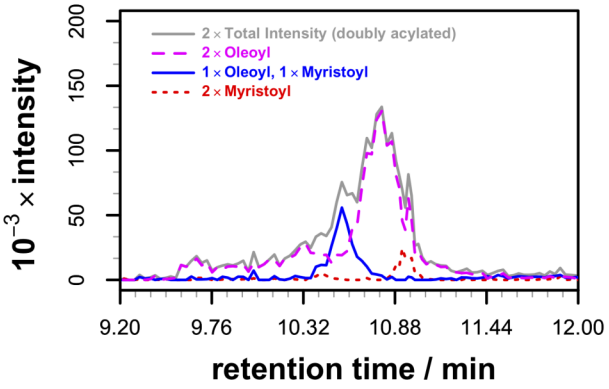

Fig. S12 Total and extracted ion intensities (absolute values) for doubly acylated melittin in the reaction with DMPG/DOPC after 52 h.

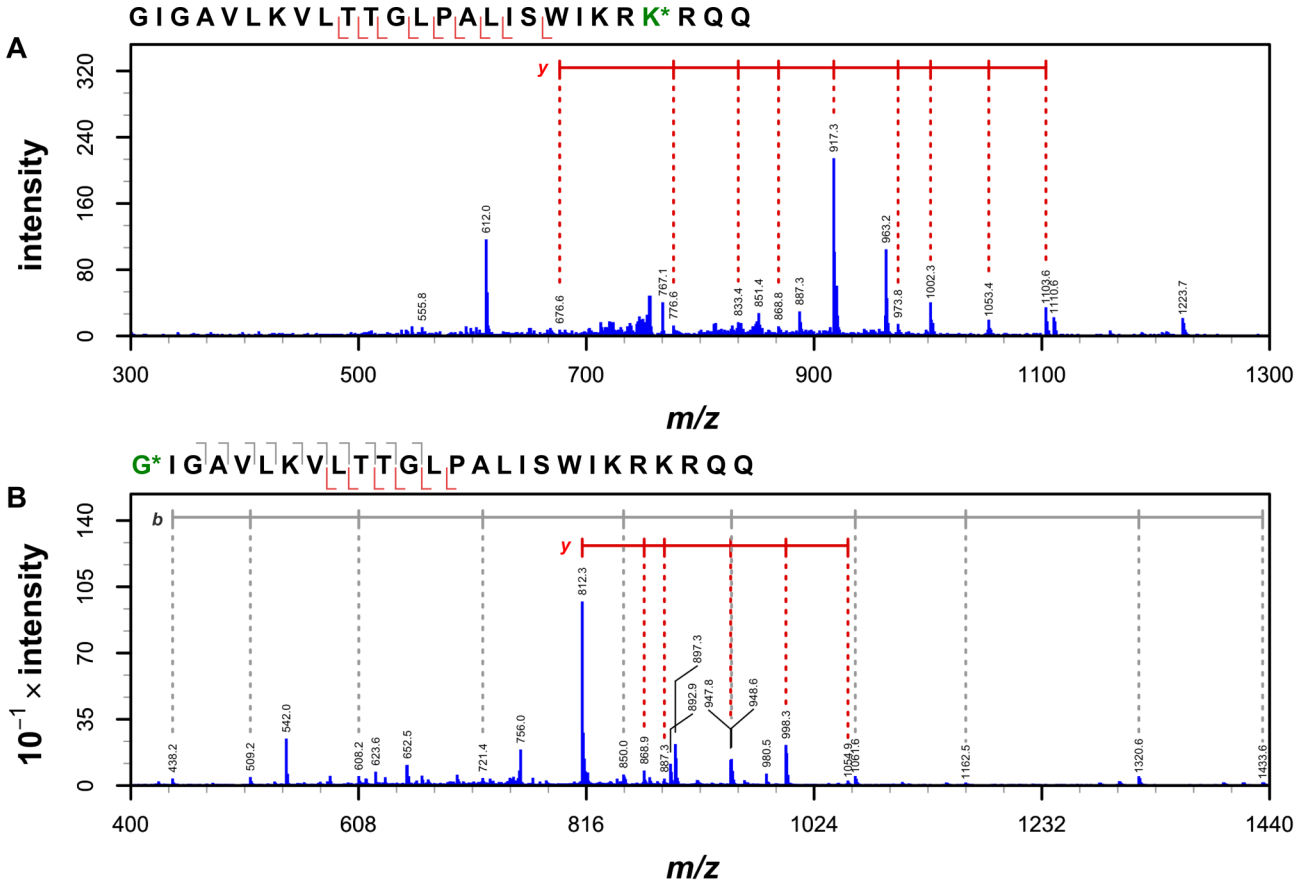

Fig. S13 MS/MS spectra (absolute intensities) for key peaks in the LC-MS chromatogram for the reaction of melittin with DOPC/DMPG (Fig. 9, main paper): (A) peak iii, precursor ion *m/z* 765.0; (B) peak iv, precursor ion *m/z* 765.0. Residues (G*, K*) matching the site of modification are indicated by asterisks. Full assignments are given in Tables S14 and S15.

Table S14 Assignments for ions in the MS/MS spectrum of peak iii in the DMPG/DOPC LC chromatogram (Fig. 9 main paper), precursor ion *m/z* 765. Assignments correspond to Fig. S13(A).

ion	Obs. *m/z*	*z*	sequence[a]
y_8	676.6	2	WIKRKRQQ-NH_2 [1×Myr]
y_9	720.3	2	SWIKRKRQQ-NH_2 [1×Myr]
y_{10}	776.6	2	ISWIKRKRQQ-NH_2 [1×Myr]
y_{11}	833.4	2	LISWIKRKRQQ-NH_2 [1×Myr]
y_{12}	868.8	2	ALISWIKRKRQQ-NH_2 [1×Myr]
y_{13}	917.3	2	PALISWIKRKRQQ-NH_2 [1×Myr]
y_{14}	973.8	2	LPALISWIKRKRQQ-NH_2 [1×Myr]
y_{15}	1002.3	2	GLPALISWIKRKRQQ-NH_2 [1×Myr]
y_{16}	1053.4	2	TGLPALISWIKRKRQQ-NH_2 [1×Myr]
y_{17}	1103.6	2	TTGLPALISWIKRKRQQ-NH_2 [1×Myr]
y_{18}	1160.0	2	LTTGLPALISWIKRKRQQ-NH_2 [1×Myr]
y_{24}	963.2	3	GAVLKVLTTGLPALISWIKRKRQQ-NH_2 [1×Myr]
y_{21}	887.3	3	LKVLTTGLPALISWIKRKRQQ-NH_2 [1×Myr]
y_{13}	612.0	3	PALISWIKRKRQQ-NH_2 [1×Myr]
y_{11}	555.8	3	LISWIKRKRQQ-NH_2 [1×Myr]
b_9	851.4	1	GIGAVLKVL
b_{11}	1053.4	1	GIGAVLKVLTT
b_{12}	1110.5	1	GIGAVLKVLTTG
b_{13}	1223.7	1	GIGAVLKVLTTGL

[a] Key: Myr, myristoyl

Table S15 Assignments for ions in the MS/MS spectrum of peak iv in the DMPG/DOPC LC chromatogram (Fig. 9 main paper) precursor ion *m/z* 765. Assignments correspond to Fig. S13(B).

ion	Obs. *m/z*	*z*	sequence[a]
y_9	615.2	2	SWIKRKRQQ-NH_2
y_{10}	671.5	2	ISWIKRKRQQ-NH_2
y_{11}	728.1	2	LISWIKRKRQQ-NH_2
y_{13}	812.3	2	PALISWIKRKRQQ-NH_2
y_{14}	868.9	2	LPALISWIKRKRQQ-NH_2
y_{15}	897.3	2	GLPALISWIKRKRQQ-NH_2
y_{16}	947.8	2	TGLPALISWIKRKRQQ-NH_2
y_{17}	998.3	2	TTGLPALISWIKRKRQQ-NH_2
y_{18}	1054.9	2	LTTGLPALISWIKRKRQQ-NH_2
y_{12}[b]	509.2	3	ALISWIKRKRQQ-NH_2
y_{13}	542.0	3	PALISWIKRKRQQ-NH_2
y_{14}	579.5	3	LPALISWIKRKRQQ-NH_2
y_{15}	598.4	3	GLPALISWIKRKRQQ-NH_2
y_{16}	632.4	3	TGLPALISWIKRKRQQ-NH_2
y_{17}	665.9	3	TTGLPALISWIKRKRQQ-NH_2
y_{18}	703.7	3	LTTGLPALISWIKRKRQQ-NH_2
y_{20}	779.4	3	KVLTTGLPALISWIKRKRQQ-NH_2
y_{22}[b]	850.0	3	VLKVLTTGLPALISWIKRKRQQ-NH_2
y_{23}	873.9	3	AVLKVLTTGLPALISWIKRKRQQ-NH_2
y_{24}	892.9	3	GAVLKVLTTGLPALISWIKRKRQQ-NH_2
y_{25}	698.1	4	IGAVLKVLTTGLPALISWIKRKRQQ-NH_2
b_3	438.2	1	GIG [1×Myr]
b_4[b]	509.2	1	GIGA [1×Myr]
b_5	608.2	1	GIGAV [1×Myr]
b_6	721.4	1	GIGAVL [1×Myr]
b_7[b]	850.0	1	GIGAVLK [1×Myr]
b_8	948.6	1	GIGAVLKV [1×Myr]
b_9	1061.6	1	GIGAVLKVL [1×Myr]
b_{10}	1162.5	1	GIGAVLKVLT [1×Myr]
b_{12}	1320.6	1	GIGAVLKVLTTG [1×Myr]
b_{13}	1433.6	1	GIGAVLKVLTTGL [1×Myr]
b_9	531.4	2	GIGAVLKVL [1×Myr]
b_{10}	582.1	2	GIGAVLKVLT [1×Myr]
b_{11}	632.4	2	GIGAVLKVLTT [1×Myr]
b_{12}	661.1	2	GIGAVLKVLTTG [1×Myr]
b_{11}-H_2O	623.6	2	GIGAVLKVLTT [1×Myr]
b_{12}-H_2O	1302.8	1	GIGAVLKVLTTG [1×Myr]
b_{12}-H_2O	652.5	2	GIGAVLKVLTTG [1×Myr]

[a] Key: Myr, myristoyl; int, internal; [b] some observed *m/z* are very close matches to ions in both b and y sequence ladders and have been included in both

Kinetics of the POPC Reaction

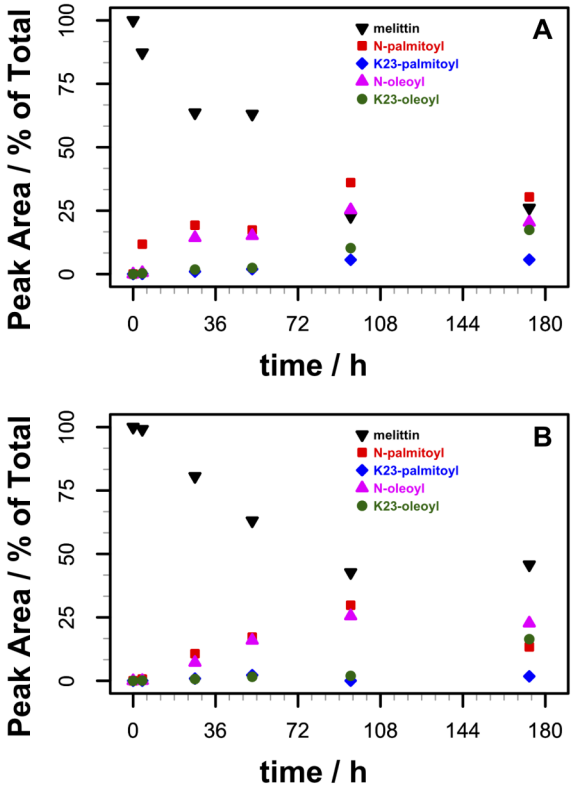

Fig. S14 Rates of formation and consumption of key species in the reaction of melittin with POPC (A) and OPPC (B). At each time point, the integrated area of each peak from the extracted ion chromatogram is determined as a percentage of the total integrated area for all peaks.

Notes and references

[a] *Department of Chemistry, Biophysical Sciences Institute, Durham University, Durham, United Kingdom. Fax: +44 (0)1913844737; Tel: +44 (0)191 3730838; E-mail: j.m.sanderson@durham.ac.uk*

1 Calculated using ProtParam (www.expasy.ch/tools/protparam.html) using a modified extinction coefficient for Trp according to Pace (C. N. Pace, F. Vajdos, L. Fee, G. Grimsley, and T. Gray, *Protein Sci.*, 1995, **11**, 2411).

2 H. P. Benton, D. M. Wong, S. A. Trauger, and G. Siuzdak, *Anal. Chem.*, 2008, **80**, 6382–6389.

3 R Development Core Team R: A language and environment for statistical computing, R Foundation for Statistical Computing, Vienna, Austria, 2008. (ISBN 3-900051-07-0, URL http://www.R-project.org).